2010 IEEE International Conference on Robotics and Automation
Anchorage Convention District
May 3-8, 2010, Anchorage, Alaska, USA

Adaptive formation control of a fleet of mobile robots: Application to autonomous field operations.

Roland Lenain*, Johan Preynat*, Benoit Thuilot†, Pierre Avanzini†, Philippe Martinet†

* Cemagref
24, av. des Landais
63172 Aubière Cedex France
roland.lenain@cemagref.fr

† LASMEA
24, av. des Landais
63177 Aubière Cedex France
benoit.thuilot@lasmea.univ-bpclermont.fr

***Abstract*— The necessity of decreasing the environmental impact of agricultural activities, while preserving in the same time the level of production to satisfy the growing population demand, requires to investigate new production tools. Mobile robotic can constitute a promising solution, since autonomous devices may permit to increase production level, while reducing pollution thanks to a high accuracy. In this paper, the use of several mobile robots for field treatment is investigated. It is here considered that they can exchange data through wireless communication, and a formation control law, accurate despite typical off-road conditions (low grip, terrain irregularities, etc), is designed relying on nonlinear observer-based adaptive control. The algorithm proposed in this paper is tested through advanced simulations in order to study separately its capabilities, as well as experimentally validated.**

I. INTRODUCTION

The continuous advances in autonomous mobile robot control (concerning both a single robot [4], as well as multi-robots [1], [7]) offer new possibilities in terms of applications for every-day life improvement. For instance, the development of automated multi-robot fleets can benefit to many applications requiring to cover large areas [5], such as surveillance, cleaning, exploration, etc. It is particularly interesting in environmental applications such as farming, where the use of several light robots in the field may permit to reduce environmental impact while preserving the level of production. This constitutes a challenging problem as stated in [2]. Rather than considering numerous small robots, as in swarm robotics [12], a cooperation framework with a limited number of light machines seems preferable when field treatment is addressed : on one hand, some farming operations such as harvesting require quite large machines to achieve tasks properly, and on the other hand, it appears more tractable from a practical point of view (maintenance, monitoring, acceptability, etc). As a consequence, this paper is focused on formation control of several light robots executing operations in field (as illustrated in figure 1), allowing the use of several autonomous entities instead of driving a sole huge vehicle.

In the considered applications, a reference path is defined by the leader vehicle, controlled either manually or autonomously. The shape of the formation is not considered as fixed, since the area covering may require a varying formation (tank unload, maneuvers, etc). Several approaches have been proposed for mobile robot formation control [8], [14], but they are mainly dedicated to structured environments. In contrast, the context of the considered tasks requires a high accurate relative positioning of the robots despite the numerous perturbations encountered in natural environment (skidding, terrain irregularities, etc). This is not addressed by classical approaches.

In this paper, an adaptive algorithm for formation control is proposed, relying on a reference trajectory defining a local relative frame. It decouples longitudinal and lateral dynamics with respect to the desired path : the advance of each robot along the reference path can be addressed independently from the regulation of its lateral deviation with respect to this path. Longitudinal control is based on the regulation of curvilinear inter-vehicle distances, while lateral regulation relies on an observer-based adaptive control approach. The control of the possibly varying formation gathers both control laws, enabling an accurate formation regulation for field operations, independently from the reference path shape and environment properties.

Fig. 1. Illustration of the application

The paper is organized as follows : a model dedicated to a mobile robot formation is firstly introduced, together with the observation strategy allowing to reflect the bad grip conditions encountered in natural environment. Based on this model, the control of each mobile robot is then detailed : longitudinal control is recalled from previous work, while lateral control is designed with respect to a varying set point. The validation of the proposed control is finally achieved thanks to advanced simulations and actual experiments (limited in this paper to urban mobile robots).

II. MOBILE ROBOT MODELING

The autonomous control of a fleet of mobile robots is considered with respect to a desired path, used as a reference frame for both longitudinal and lateral positioning of each robot. The objective is to ensure an accurate overall motion of the robots in a desired, but potentially varying, configuration along this chosen trajectory. The control problem investigated

in this paper then derives from the path tracking one. The following framework for formation control is consequently introduced.

A. Model of a robot formation

The overall control strategy for the robot formation is based on the modeling proposed in figure 2 (two robots among n are shown).

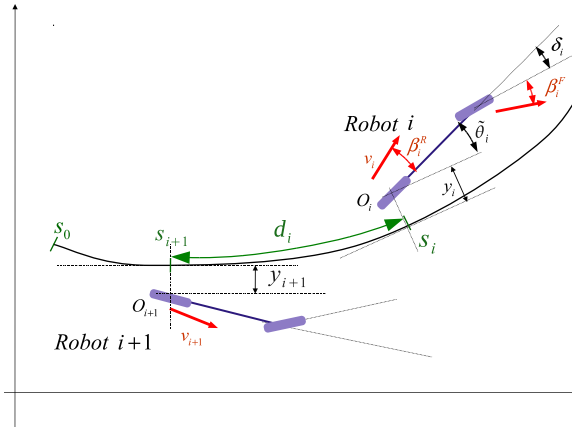

Fig. 2. Longitudinal model of a robot fleet

In this representation, each robot is viewed as a bicycle, as in the celebrated Ackermann model, see [13] : an unique wheel for the front axle and another one for the rear axle. The classical rolling without sliding assumption is not satisfied in a natural context. As they affect significantly robot dynamics, low grip conditions depreciate the path tracking accuracy. In order to account for this specificity, two sideslip angles are added : β^F and β^R, respectively for front and rear axles. Their estimation is described in section II-B. These variables are representative of the difference between the tire orientation and the actual tire speed vector direction. Longitudinal sliding has not been described, since in the considered applications, longitudinal guidance accuracy is not as critical as lateral one. Based on these assumptions, the notations used in the sequel are depicted in figure 2 for the i^{th} robot and hereafter listed :

- Γ is the common reference path for each robot defined in an absolute frame (computed or recorded beforehand).
- O_i is the center of the i^{th} mobile robot rear axle. It is the point to be controlled for each robot.
- s_i is the curvilinear coordinate of the closest point from O_i belonging to Γ. It corresponds to the distance covered along Γ by robot i.
- $c(s_i)$ denotes the curvature of path Γ at s_i.
- $\tilde{\theta}_i$ denotes the angular deviation of robot i w.r.t. Γ.
- y_i is the lateral deviation of robot i w.r.t. Γ.
- δ_i is the i^{th} robot front wheel steering angle.
- l is the robot wheelbase.
- v_i is the i^{th} robot linear velocity at point O_i.
- β_i^F and β_i^R denote the sideslip angles (front and rear) of the i^{th} robot.

Using these notations, the motion equations for the i^{th} mobile robot can be expressed as (see [9] for details) :

$$\begin{aligned} \dot{s}_i &= v_i \frac{\cos(\tilde{\theta}_i+\beta_i^R)}{1-c(s_i)\,y_i} \\ \dot{y}_i &= v_i \sin(\tilde{\theta}_i+\beta_i^R) \\ \dot{\tilde{\theta}}_i &= v_i \left(\cos\beta_i^R \frac{\tan(\delta_i+\beta_i^F)-\tan(\beta_i^R)}{l} - \frac{c(s_i)\,\cos\tilde{\theta}_i}{1-y_i\,c(s_i)}\right) \end{aligned} \quad (1)$$

Expression (1) does not exist if $[\,1-c(s_i)y_i\,]=0$ (i.e. point O_i is superposed with the instantaneous reference path center of curvature). Such a situation is not encountered in practice, since robots are supposed to be properly initialized. The state vector for robot i is then defined as $X_i=[s_i \;\; y_i \;\; \tilde{\theta}_i]^T$, and is supposed to be measured. As a result, model (1) is entirely known as soon as sideslip angles β_i^F and β_i^R are accessible. As these variables cannot be easily measured, they are estimated thanks to an observer described below.

B. Sideslip angle estimation

As sideslip angles integrated into robot model (1) are hardly measurable directly, their indirect estimation has to be addressed. The observer-based approach detailed in [6] is here implemented. It follows the algorithm described in figure 3, taking benefit of the duality principle between observation and control.

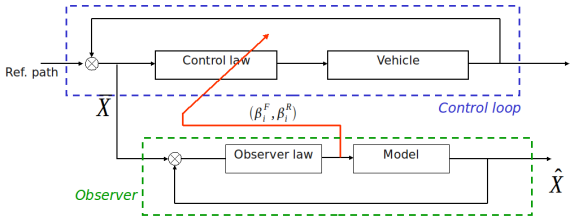

Fig. 3. Observer principle scheme

More precisely, model (1) is considered as a process to be regulated thanks to sideslip angles. The observer consists then in a control law designed for these sideslip angles, with the aim to ensure the convergence of some model outputs ($X_i^{obs}=[y_i^{obs} \;\; \tilde{\theta}_i^{obs}]^T$) with the corresponding measured ones ($\bar{X}_i=[\bar{y}_i \;\; \bar{\tilde{\theta}}_i]^T$). Such a convergence ensures that model (1) is representative of vehicle actual behavior, whatever the grip conditions, and sideslip angle values can then be reported into mobile robot control laws. The detailed computation of this observer and proofs of stability are available in [6].

C. Model exact linearization for control

Kinematic model (1) has been extended to account for low grip conditions. Nevertheless, it is still consistent with classical kinematic models, such as considered in [13]. It can consequently be turned into a chained form, enabling then an exact linearization. This can be achieved by imposing the following invertible state and control transformations :

$$\begin{aligned} [s_i, y_i, \tilde{\theta}_i] \;\rightarrow\; & [a_{1i}, a_{2i}, a_{3i}] = \\ & [s_i, y_i, (1-c(s_i)\,y_i)\tan(\tilde{\theta}_i+\beta_i^R)] \\ [v_i, \delta_i] \;\rightarrow\; & [m_{1i}, m_{2i}] = [\tfrac{v_i\cos(\tilde{\theta}+\beta_i^R)}{1-c(s_i)\,y_i}, \tfrac{da_{3i}}{dt}] \end{aligned} \quad (2)$$

which turn system (1) into system (3).

$$\begin{cases} \dot{a}_{1i} = \frac{d\,a_{1i}}{dt} &= m_{1i} \\ \dot{a}_{2i} = \frac{d\,a_{2i}}{dt} &= a_{3i} m_{1i} \\ \dot{a}_{3i} = \frac{d\,a_{3i}}{dt} &= m_{2i} \end{cases} \quad (3)$$

Let us now consider, in system (3), the derivative with respect to curvilinear abscissa, instead of the derivative with respect to time. This leads finally to system (4) :

$$\begin{cases} a'_{2i} &= \frac{d\,a_{2i}}{ds_i} &= a_{3i} \\ a'_{3i} &= \frac{d\,a_{3i}}{ds_i} &= m_{3i} = \frac{m_2 i}{m_1 i} \end{cases} \quad (4)$$

which constitutes an exact linear form. Since $a_{1i} = s_i$, then $a'_{1i} = 1$ and is consequently removed from the model, which is then unchanged whatever the robot velocity. As a result, these transformations permit to separate formally the robot longitudinal behavior from its lateral motion with respect to the path to be followed. Both longitudinal and lateral control can then be addressed independently.

III. Mobile robot formation control

To address the control of a fleet of mobile robots in a path tracking context, the relative positioning of each robot with respect to the reference trajectory is achieved and then shared within the fleet via wireless communication. The control of each robot aims then at ensuring the convergence to desired set points in terms of curvilinear offset (longitudinal control) and lateral deviation offset (lateral control). In the sequel, the longitudinal control issued from previous work is briefly described. Then, the lateral control law, constituting the main contribution of this paper, is detailed.

A. Longitudinal control law

The objective of longitudinal control is to maintain a desired distance (denoted d) between curvilinear abscissas of successive vehicles. Preferentially, each robot is controlled with respect to the curvilinear abscissa s_1 of the leader (1^{st} vehicle). This enables to avoid an oscillating behavior due to error propagation along the fleet. However, for obvious safety reasons, the distance to the previous vehicle has also to be considered. Therefore, as proposed in [3], a composite error x_i equal to the distance to the leader vehicle e_i^1 in the nominal case, and smoothly commuting to the distance to the preceding vehicle e_i^{i-1} when the security distance is approached, is here regulated, see figure 4. The auxiliary control m_{1i} (and therefore v_i) ensuring that x_i converges with zero can easily be designed from the first equation in model (3), so that each vehicle can be accurately and safely controlled longitudinally, whatever the velocity of the leader.

B. Lateral control law

1) Lateral desired set point: Once longitudinal control has been achieved, the control of the lateral position of each robot can be addressed. In contrast to the classical path tracking problem, where the tracking error is expected to be null [11], the lateral deviation of each robot in a formation has to converge to a non-null desired set point. To this aim, the model is extended with a new variable $y_i^d(s_i)$, representative of the desired lateral deviation of robot i, and permitting the relative positioning of mobile robots in 2D space, see figure 5.

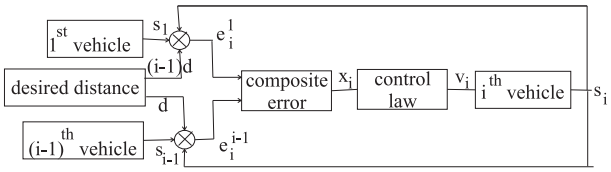

Fig. 4. Longitudinal control scheme

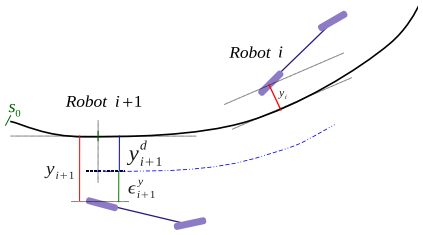

Fig. 5. Lateral control model

2) Control law design: Relying on linear system (4) derived from state transformations (2), the goal of lateral control consists in regulating $a_{2i} = y_i$ to a desired set point : $y_i \rightarrow y_i^d$. This objective can be achieved by imposing the virtual control law (5) for m_{3i} :

$$m_{3i} = -K_d(a_{3i} - y_i'^d) - K_p(a_{2i} - y_i^d) + y_i''^d \quad (K_d, K_p > 0) \quad (5)$$

This indeed leads to the following second order differential equation satisfied by the regulation error of the i^{th} robot, denoted $\epsilon_i^y = a_{2i} - y_i^d$:

$$\epsilon_i''^y + K_d \epsilon_i'^y + K_p \epsilon_i^y = 0 \quad (6)$$

which ensures the convergence of ϵ_i^y to zero (i.e : $y_i \rightarrow y_i^d$).

The steering control law of robot i can then be deduced from the virtual control m_{3i} thanks to the inverse transformations (2). It leads (if $\epsilon_i''^y$ is neglected) to :

$$\delta_i = \arctan\left\{ \tan(\beta_i^R) + \frac{l}{\cos(\beta_i^R)} \left(\frac{c(s_i)\cos\tilde{\theta}_{2i}}{\alpha_i} + \ldots \right. \right. \\ \left. \left. \ldots \frac{A_i \cos^3\tilde{\theta}_{2i}}{\psi \alpha_i^2} \right) \right\} + \beta_i^F \quad (7)$$

with :

$$\begin{cases} \tilde{\theta}_{2i} &= \tilde{\theta} + \beta_i^R \\ \alpha_i &= 1 - c(s_i) y_i \\ A_i &= -K_p \epsilon_i^y - K_d\, \alpha_i\, \eta + c(s_i) \alpha_i\, \eta \tan\tilde{\theta}_{2i} \\ \eta &= (\tan\tilde{\theta}_{2i} - \frac{\dot{y}_i^d}{v_i \cos\tilde{\theta}_{2i}}) \\ \psi &= 1 + \tan^2(\tilde{\theta}_{2i}) - \frac{\dot{y}_i^d \tan\tilde{\theta}_{2i}}{v_i \cos\tilde{\theta}_{2i}} \end{cases} \quad (8)$$

Control law (8) exists under the following assumptions :

- the longitudinal acceleration can be neglected ($\dot{v}_i = 0$). The gains of the longitudinal control law can be tuned

to meet this assumption, while keeping a satisfactory longitudinal behavior

- $1 - c(s_i)y_i \neq 0$: model existence condition, already discussed.
- $\tilde{\theta}_{2i} \neq \frac{\pi}{2}[\pi]$, i.e. the rear robot speed vector is not perpendicular to the path to be followed. It is satisfied when the formation is properly initialized.

In the same way that d permits to define the distance between robots within the fleet and then their relative longitudinal positions, the variable y_i^d in (7) permits to define their lateral positions with respect to the global formation motion. Longitudinal and lateral relative positions of each robot can then be specified in the reference trajectory frame independently. The set point y_i^d has now to be constructed to regulate a desired formation, in order to achieve a multi-robot task.

3) Generation of desired set point: When achieving a field treatment with several machines, the desired lateral distance between the tracks of each vehicle is chosen as the implement width, usually reduced with 15% in order to have a small overlapping margin to ensure a proper field covering. Just as in the longitudinal case, in order to avoid an oscillating behavior due to error propagation along the fleet, each robot must preferentially be controlled with respect to the leader trajectory. This can easily be achieved by specifying a constant y_i^d in (7). This first mode is completely satisfactory as long as vehicles are never side-by-side (e.g. when field treatment is achieved according to a winger configuration).

Mode 1 (fixed inter-track) : $y_i^d(s_i) = d_i^y$, *with* d_i^y *a constant chosen w.r.t. implement widths. The lateral position of a robot is independent from previous robot behaviors and does not repeat their possible deviations.*

In contrast, when robots have to work side-by-side (e.g. a farm tractor moving alongside a combine harvester to unload it), robot i must reproduce robot $i-1$ deviation in order to enable joint work (e.g. unloading) and avoid collision. Ideally, as long as robot $i-1$ deviation does not exceed some pre-specified threshold, robot i should be controlled with respect to the leader trajectory, in order to avoid the above mentioned oscillating behavior due to error propagation, and when the threshold is exceeded, then robot i should be controlled with respect to robot $i-1$ trajectory. Such a behavior can actually be imposed, since the desired lateral set point $y_i^d(s_i)$, introduced in figure 5, may be varying. For this second mode, it is here proposed to design $y_i^d(s_i)$ as :

$$y_i^d(s_i) \quad = \quad d_i^y + \sigma(y_{i-1})\,[\,y_{i-1} - d_{i-1}^y\,] \qquad (9)$$

where $\sigma(y_{i-1}) \in [\,0\,;\,1\,]$ is the smooth commutation function shown in figure 6 : if y_{i-1} is small, then $\sigma(y_{i-1}) = 0$, so that $y_i^d(s_i) = d_i^y$ as in the first mode. In contrast, if y_{i-1} is large, then $\sigma(y_{i-1}) = 1$, so that robot i lateral objective is to reproduce robot $i-1$ lateral deviation.

Mode 2 (adapted inter-track) : $y_i^d(s_i)$ *is defined by (9)*
Robot i *reproduces robot* $i-1$ *deviation, if the latter exceeds a pre-specified threshold.*

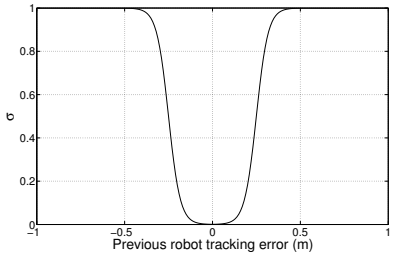

Fig. 6. Shape of commutation function

IV. Simulation results

In order to validate theoretically the proposed algorithm and investigate its robustness with respect to sliding phenomena, simulated results obtained with MATLAB/Simulink coupled to multi-body dynamic simulation software Adams are here reported. Such a simulation testbed permits to render accurately the behavior of actual mechanical systems. In particular, the specificities of mobile robot motion in natural environment can be emulated (grip conditions, ground irregularities, low-level settling time, etc). In order to investigate the capabilities of the proposed algorithm, three mobile robots have been designed (as depicted in figure 7(a)) and a soil with low grip conditions (equivalent to wet grass) has been parameterized. Delays and settling times of the actuators are also accounted : 500ms for the steering actuator and 700ms for the velocity actuator, corresponding to the values measured on available experimental robots. A reference path consisting in an U-turn has been computed, such as depicted in figure 7(b) in black plain line. It has to be followed by the leader at a $3m.s^{-1}$ velocity, and the desired distance between robots has been set to $d = 5.5\ m$.

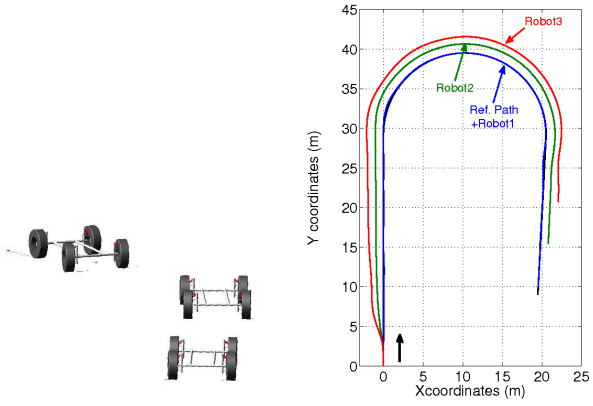

(a) Virtual mobile robots (b) Reference trajectory

Fig. 7. Simulation testbed

The objective of the three simulated robots, as well as their control parameters, are described below :

- Leader : no lateral deviation is specified (i.e. $y_1^d = 0$), and the control law accounting for sliding is used.

- Robot 2 (first follower) : mode 1 has been considered, i.e. a constant desired lateral deviation $y_2^d = d_2^y = -1m$ has been specified. Moreover, in order to demonstrate the influence of sliding, the sideslip angle estimation has been frozen, i.e. $(\beta_2^F, \beta_2^R) = (0, 0)$.
- Robot 3 (second follower) : mode 2 has been considered, i.e. a composite objective has been specified with $d_3^y = -2m$. The control law accounting for sliding is used, in order to show how robot 3 reacts to robot 2 large tracking error (following from sliding phenomenon encountered during the curve).

Global trajectories achieved by each robot are superposed in figure 7(b). Next, the lateral deviations of the three robots recorded during this test are reported in figure 8.

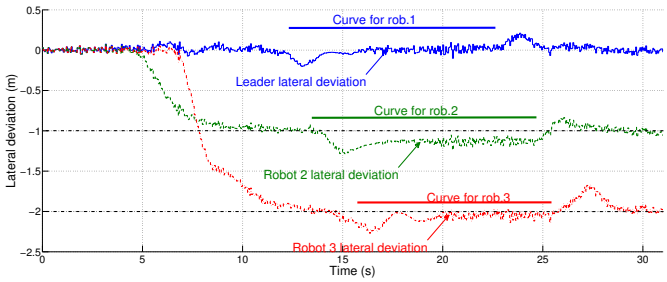

Fig. 8. Lateral deviations recorded in simulation

The leader tracking error, depicted in blue plain line, is satisfactorily regulated to zero with an accuracy inferior to $10cm$, despite the bad grip conditions. A $20cm$ overshoot can nevertheless be observed at the beginning and at the end of the curve (times $13s$ and $23s$), due to the settling time of the simulated actuator.

On the contrary, the second mobile robot is unable to achieve its objective with such an accuracy : during the straight line parts of the trajectory (before $14s$ and after $24s$), robot 2 accurately reaches the expected -$1m$ deviation. However, during the curve, it converges with a -$1.2m$ constant lateral deviation (i.e. ϵ_2^y=$20cm$) because of the bad grip conditions : sideslip angle estimated values are indeed around 3°, which is consistent with what is recorded in actual experiments, see [10]. This proves that sliding phenomenon, when not reported in control laws as it is the case for robot 2, significantly depreciates lateral guidance accuracy.

Finally, since sliding phenomenon is accounted in robot 3 control laws, this robot could have accurately met its objective. However, since mode 2 has been considered and robot 2 lateral deviation is large during the curve, robot 3 lateral objective has been adapted : ϵ_2^y=$20cm$ corresponds to the center of the transition part in the commutation function, see figure 6. Consequently, y_3^d is shifted to -$2.1m$ instead of -$2m$, and it can be observed that robot 3 lateral deviation satisfactorily converges with this adapted objective during the curve. Of course, when the curve is over (after time $27s$), robots no longer undergo sliding phenomenon : robot 2 lateral deviation then goes back to its objective, and so does robot 3 lateral deviation.

These results demonstrate the capabilities of the algorithm in accurately controlling a formation, despite sliding phenomenon. It also shows the ability of mode 2 (adapted inter-track) to manage on-line formation reconfiguration.

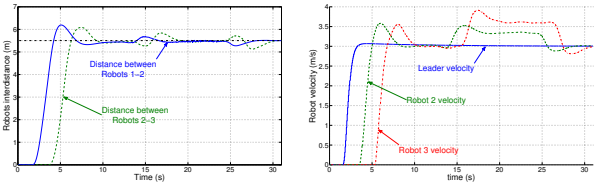

(a) Distances between robots (b) Mobile robot velocities

Fig. 9. Simulation results on longitudinal servoing during simulation

The longitudinal performances are investigated in figure 9. The distances between robots (reported in figure 9(a)) show that the $5.5m$ objective is satisfactorily obtained, despite skidding and variations in the curvature (robots 2 and 3 have a larger targeted curvature since they are on the external part of the curve, as pointed out in figure 7(b)). In the same way than for lateral behavior, some overshoots can be recorded when each robot enters into the curve, due to the low-level settling time. Since mobile robots 2 and 3 are on the external part of the curve, they have to increase their speed to preserve the desired inter-distance. Their velocities are compared in figure 9(b), and it can be noticed that the velocities of robot 2 and 3 present the expected behavior.

V. Experimental results

A. Experimental mobile robots and equipment

Fig. 10. Mobile robots

As a first step, prior to full-scale experiments with agricultural vehicles operating off-road, the proposed approach has been implemented on the electric vehicles Cycab shown in figure 10. They are equipped with an RTK-GPS receiver supplying an absolute position information, accurate to within $2cm$. Coupled with a Kalman filter, this sensor permits also to access to vehicle heading (and consequently to the orientation error). The communication between robots is ensured thanks to a WiFi access point enabling to transfer all the data required to feed both longitudinal and lateral control laws. These robots are able to move up to $10km.h^{-1}$.

A reference trajectory has been learnt beforehand, with the leader robot manually driven. This trajectory, reported in figure 11, is composed of a straight line, followed by a curve and another part of straight line. This allows to investigate the robustness of control algorithms with respect to path shape.

This path has been followed by a fleet composed of two mobile robots. The complete control law, including sideslip angle estimation, has been used. A $1m.s^{-1}$ desired velocity

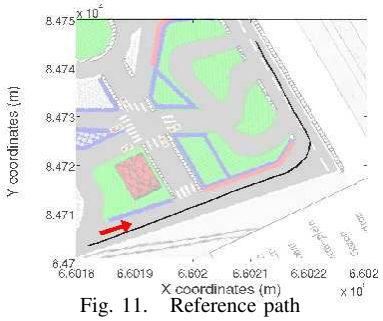

Fig. 11. Reference path

has been imposed to the leader, and an $8m$ longitudinal desired distance between the two robots has been specified. For the second robot, the lateral set point has been chosen as a sinusoidal curve, with a $0.35m$ variation range and a $10.5m$ period w.r.t. the curvilinear abscissa. This objective is consistent with the vehicle steering angle and steering rate limits. Such an experiment is not representative for a specific agricultural task, but it permits to clearly investigate the capabilities of the proposed algorithm when the lateral set point is varying.

B. Validation with a varying lateral set point

The results regarding lateral regulation are reported in figure 12. The desired sinusoidal error is reported in green dotted line, while the actual follower's error during the test is depicted in red dashed line[1].

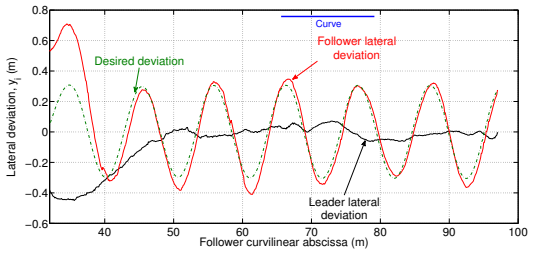

Fig. 12. Lateral deviations obtained during the experiment

It can be noticed that, even when the lateral set point is always varying, the difference between desired and actual deviations stay quite small (below $10cm$) all along the trajectory tracking and whatever the trajectory shape. The accuracy level is indeed not altered in the curve : the lateral deviation error is unchanged between curvilinear abscissas $65m$ to $78m$. Finally, the tracking error of the leader is reported in black plain line in the same figure. It can be seen that its lateral error stays below $10cm$, even during the curve, showing the relevance of the path tracking algorithm.

VI. CONCLUSION AND FUTURE WORKS

This paper proposes an algorithm for the accurate control of a mobile robot formation moving off-road. This approach considers the formation control as the combination of (i) a platooning control and (ii) an extension of the path tracking problem to a non-null lateral deviation regulation. As a result, the control of each vehicle is decomposed into longitudinal and lateral control with respect to a reference path. An adaptive control strategy allows to take into account for low grip conditions, as well as other phenomena encountered off-road and depreciating the accuracy of classical algorithms. The relative positioning of each robot with respect to a possibly varying formation can then be regulated with a few centimeter accuracy, whatever the shape of the reference trajectory and the grip conditions. The efficiency of the approach has been tested through actual experiments with two urban mobile robots.

The efficiency of the control algorithm with respect to sliding phenomena has been checked in advanced simulations and must now be validated by experimental tests with off-road mobile platforms. In addition, the proposed strategy is focused on the regulation of a formation with respect to a reference trajectory supplied beforehand. Such an algorithm has now to be extended in order to manage automatically the formation (modification of the formation, mobile robot entering/leaving the fleet, obstacle avoidance, etc).

[1] Videos of this test and another test with a constant desired lateral deviation are available on the site : ftp ://ftp.clermont.cemagref.fr/pub/Tscf/Lenain/VideoIcra2010/

REFERENCES

[1] T. Balch and R. Arkin, *Behavior-based formation control for multi-robot teams*, IEEE Transactions on Robotics and Automation **14(6)** (1998), 926–939.

[2] S. Blackmore, B. Stout, M. Wang, and B. Runov, *Robotic agriculture - the future of agricultural mechanisation ?*, 5th European Conference on Precision Agriculture (ECPA), Upsala (Sweden) (2005).

[3] J. Bom, B. Thuilot, F. Marmoiton, and P. Martinet, *A global control strategy for urban vehicles platooning relying on nonlinear decoupling laws*, IEEE/RSJ International Conference on Intelligent Robots and Systems (IROS), Edmonton (Canada), 2005, pp. 2875–2880.

[4] C. Canudas de Wit, G. Bastin, and B. Siciliano, *Theory of robot control*, Springer-Verlag, New York, USA, 1996.

[5] Y. Cao, A. Fukunaga, and A. Kahng, *Cooperative mobile robotics : Antecedents and directions*, Autonomous Robots **4(1)** (1997), 7–27.

[6] C. Cariou, R. Lenain, B. Thuilot, and M. Berducat, *Automatic guidance of a four-wheel-steering mobile robot for accurate field operations*, Journal of Field Robotics **26(6-7)** (2009), 504–518.

[7] J. Desai, J. Ostrowski, and V. Kumar, *Controlling formations of multiple mobile robots*, IEEE International Conference on Robotics and Automation (ICRA), Leuven (Belgium), 1998, pp. 2864–2869.

[8] J. Fax and R. Murray, *Information flow and cooperative control of vehicle formations*, IEEE Transactions on Automatic Control **49(9)** (2004), 1465–1476.

[9] R. Lenain, B. Thuilot, C. Cariou, and P. Martinet, *High accuracy path tracking for vehicles in presence of sliding. application to farm vehicle automatic guidance for agricultural tasks*, Autonomous robots **21(1)** (2006), 79–97.

[10] ———, *Mixed kinematic and dynamic sideslip angle observer for accurate control of fast off-road mobile robots*, Journal of Field Robotics **27(2)** (2009), 181–196.

[11] P. Morin and C. Samson, *Commande de véhicules sur roues non holonomes, une synthèse.*, Actes des troisièmes journées nationales de la recherche en robotique (JNRR), Giens (France), 2001.

[12] E. Sahin, *Swarm robotics : from sources of inspiration to domains of application*, Swarm Robotics, Proceedings of the SAB 2004 International Workshop, Lecture Notes in Computer Science (2004).

[13] C. Samson, *Control of chained systems. application to path following and time-varying point stabilization of mobile robots*, IEEE Transactions on Automatic Control **40(1)** (1995), 64–77.

[14] H. Yamaguchi, T. Arai, and G. Beni, *A distributed control scheme for multiple robotic vehicles to make group formations*, Robotics and Autonomous Systems **36(4)** (2001), 125–147.